NEOPLASIA
www.neoplasia.com

Volume 13 Number 9 September 2011 pp. 784–791 784

Invasion Precedes Tumor Mass Formation in a Malignant Brain Tumor Model of Genetically Modified Neural Stem Cells[1,2]

Oltea Sampetrean[*,†], Isako Saga[*,‡], Masaya Nakanishi[*,§], Eiji Sugihara[*,†], Raita Fukaya[‡], Nobuyuki Onishi[*], Satoru Osuka[*,¶], Masaki Akahata[*,#], Kazuharu Kai[*], Hachiro Sugimoto[§], Atsushi Hirao[**] and Hideyuki Saya[*,†]

*Division of Gene Regulation, School of Medicine, Keio University, Tokyo, Japan; †Core Research for Evolutional Science and Technology, Japan Science and Technology Agency, Tokyo, Japan; ‡Department of Neurosurgery, School of Medicine, Keio University, Tokyo, Japan; §Department of Neuroscience for Drug Discovery, Graduate School of Pharmaceutical Sciences, Kyoto University, Kyoto, Japan; ¶Department of Neurosurgery, Institute of Clinical Medicine, Graduate School of Comprehensive Human Sciences, University of Tsukuba, Ibaraki, Japan; #Second Department of Neurosurgery, Faculty of Medicine, Toho University, Tokyo, Japan; **Division of Molecular Genetics, Cancer Research Institute, Kanazawa University, Ishikawa, Japan

Abstract

Invasiveness, cellular atypia, and proliferation are hallmarks of malignant gliomas. To effectively target each of these characteristics, it is important to understand their sequence during tumorigenesis. However, because most gliomas are diagnosed at an advanced stage, the chronology of gliomagenesis milestones is not well understood. The aim of the present study was to determine the onset of these characteristics during tumor development. Brain tumor–initiating cells (BTICs) were established by overexpressing H-Ras^{V12} in normal neural stem/progenitor cells isolated from the subventricular zone of adult mice harboring a homozygous deletion of the *Ink4a/Arf* locus. High-grade malignant brain tumors were then created by orthotopic implantation of 10^5 BTICs into the forebrain of 6-week-old wild-type mice. Mice were killed every week for 5 weeks, and tumors were assessed for cellular atypia, proliferation, hemorrhage, necrosis, and invasion. All mice developed highly invasive, hypervascular glioblastoma-like tumors. A 100% penetrance rate and a 4-week median survival were achieved. Tumor cell migration along fiber tracts started within days after implantation and was followed by perivascular infiltration of tumor cells with marked recruitment of reactive host cells. Next, cellular atypia became prominent. Finally, mass proliferation and necrosis were observed in the last stage of the disease. Video monitoring of BTICs in live brain slices confirmed the early onset of migration, as well as the main cell migration patterns. Our results showed that perivascular and intraparenchymal tumor cell migration precede tumor mass formation in the adult brain, suggesting the need for an early and sustained anti-invasion therapy.

Neoplasia (2011) 13, 784–791

Abbreviations: BTIC, brain tumor–initiating cell; NSC/NPCs, neural stem/progenitor cells; Ras-NSC, neural stem cells transduced with H-Ras^{V12}; SVZ, subventricular zone

Address all correspondence to: Hideyuki Saya, MD, PhD, Division of Gene Regulation, Institute for Advanced Medical Research, Keio University School of Medicine, 35 Shinanomachi, Shinjuku-ku, Tokyo 160-8582, Japan. E-mail: hsaya@a5.keio.jp

[1]This study was supported by a Ministry of Education, Culture, Sports, Science, and Technology of Japan grant to H.S.
[2]This article refers to supplementary materials, which are designated by Videos W1 to W4 and Figure W1 and are available online at www.neoplasia.com.
Received 6 May 2011; Revised 31 July 2011; Accepted 3 August 2011

DOI 10.1593/neo.11624

Introduction

Malignant gliomas, especially glioblastomas, are most often diagnosed at an advanced stage. They show a rapid progression and quickly become lethal despite intensive treatment regimens. By the time of initial surgical evaluation, most malignant gliomas, particularly primary glioblastomas, already exhibit pronounced cellular and histologic heterotypia, diffuse infiltration into the brain, hemorrhage, and necrosis. These histopathologic features are the only diagnostic criteria for this tumor type. Establishing the order of their appearance during tumor formation can further our understanding of disease progression and help modulate therapeutic strategies.

Although numerous preclinical models of malignant gliomas have been established, classic cell line xenograft models display limited invasiveness and heterogeneity and a variable degree of pathologic similarity to human gliomas [1–3]. Recently, new animal models were developed using glioblastoma stem cells isolated from human surgical specimens [4]. Other models that have genetically engineered neural stem cells (NSCs) and progenitor cells (NPCs) were developed [5,6]. These new models show greater similarity to human tumors [2]. However, despite improvements, long latency, variable penetrance rate, technical complexity, and/or low reproducibility are still, in many cases, precluding the systematic analysis of the characteristics of early stage glioblastoma [1].

Furthermore, to allow monitoring of disease progression, glioblastoma models should exhibit aggressive tumor formation in the adult brain in the context of an immunocompetent microenvironment. Using brain tumor–initiating cells (BTICs) genetically induced from adult murine NSCs, we established a syngeneic mouse model that consistently and faithfully recapitulates the hallmark features of glioblastomas. Our analysis of tumor progression in this model indicates that the migration of solitary tumor cells into the normal brain is the earliest event in disease progression, followed by host response, appearance of atypical cells, and mass formation.

Materials and Methods

Animal Experiments

All experiments were performed in accordance with the animal care guidelines of Keio University.

Neural Stem/Progenitor Cell Culture

Six-week-old male *Ink4a/Arf* null C57BL/6 mice (B6.129-Cdkn2atm1Rdp; National Cancer Institute, Frederick, MD) were euthanized with a lethal dose of pentobarbital. Brains were extracted, and the subventricular zone (SVZ) was isolated by microdissection, washed, trypsinized, and then mechanically dissociated. Primary NSCs/NPCs were maintained as sphere culture in Dulbecco modified Eagle medium (DMEM)/F12 (Sigma, St Louis, MO) supplemented with 20 ng/ml epidermal growth factor (EGF; PeproTech, Rocky Hill, NJ), 20 ng/ml basic fibroblast growth factor (PeproTech), B27 supplement without vitamin A (Invitrogen, Carlsbad, CA), 200 ng/ml heparan sulfate, 100 U/ml penicillin, and 100 ng/ml streptomycin (Nacalai Tesque, Kyoto, Japan) at 37°C in 5% CO_2/95% humidified air.

Retroviral Vector Constructs and Preparation of Retroviral Supernatants

Human H-Ras^{V12} cDNA [7] (kindly provided by P. P. Pandolfi) was cloned into the retroviral vector pMXs-IG (kindly provided by T. Kitamura). The empty vector was used as a control. pMXs vectors were transfected into Plat-E packaging cells [8] using FugeneHD (Roche Diagnostics, Mannheim, Germany). Medium was replaced once after 24 hours, and viral supernatants were collected and filtered with 0.45-μm cellulose acetate filters (Iwaki, Kyoto, Japan) 48 hours after transfection. Supernatants were centrifuged at 12,000*g* for 6 hours at 4°C, and the viral pellet was resuspended in small volumes of NSC culture medium.

Brain Tumor–Initiating Cells

Primary *Ink4a/Arf* null NSC/NPCs were infected with retroviral supernatants. The resulting mixture of GFP-positive and GFP-negative cells, termed *Ras-NSCs* hereafter, was cultured as spheres and used for implantation after one passage. None of the Ras-NSCs used showed any phenotypic change during culture.

Tumorsphere Culture

Primary tumors were dissected from the mouse brains and subjected to mechanical and enzymatic dissociation. GFP-positive cells were sorted from single-cell suspensions by flow cytometry (FACSVantage; Becton-Dickinson, Franklin Lakes, NJ) and cultured in NSC culture medium as tumorspheres. In all experiments, tumorspheres were dissociated to obtain a single-cell suspension before use.

Differentiation Assays

Ras-NSCs were cultured on dishes coated with poly-L-lysine (Sigma) in DMEM/F12 supplemented with 10% fetal calf serum for 2 weeks and then analyzed by immunocytochemistry.

Orthotopic Transplants

Female C57BL/6 mice aged 6 to 8 weeks were anesthetized and placed into a stereotactic apparatus equipped with a *z* axis (David Kopf Instruments, Tujunga, CA). A small hole was bored into the skull 2.0 mm lateral to the bregma using a dental drill. One hundred thousand viable cells in 2 μl of Hank's balanced salt solution were injected into the right hemisphere 3 mm below the surface of the brain using a 10-μl Hamilton syringe with an unbeveled 30-gauge needle. The injection was performed over 2 minutes, with an additional 2-minute pause before removing the syringe. The hole was sealed with bone wax, and the scalp was closed using a 9-mm autoclip applicator. Animals were followed daily for the development of neurologic deficits.

Immunohistochemistry/Immunocytochemistry

For histologic analysis, tissues were fixed overnight with 4% paraformaldehyde, embedded in paraffin and then sectioned at a thickness of 4 μm. Deparaffinized sections were stained with mouse monoclonal antibody to nestin, O4 (Millipore, Billerica, MA), rat antimouse monoclonal antibody to F4/80 (Serotec, Oxford, United Kingdom), and rabbit polyclonal antibody to GFP (Santa Cruz Biotechnology, Santa Cruz, CA), Ki67 (NeoMarkers, Fremont, CA). Immune complexes were detected with the use of M.O.M. Immunodetection Kit (Vector Laboratories, Burlingame, CA) (nestin, O4) or Histofine (Nichirei Biosciences, Tokyo, Japan) (F4/80, GFP, Ki67), and ImmPACT DAB (Vector Laboratories). For immunocytochemistry, spheres/cells were fixed with 4% paraformaldehyde and stained with mouse monoclonal antibody to nestin, O4 (Millipore), Tuj-1 (Covance, Princeton, NJ), and rabbit polyclonal antibody to GFAP (DAKO, Carpinteria, CA), followed by Alexa 568–conjugated antimouse or antirabbit IgG secondary antibody. CD44 was stained with phycoerythrin-conjugated antimouse CD44 (clone IM7; BioLegends, San Diego, CA). Nuclei were counterstained with 4′,6-diamino-2-phenylindole (DAPI, VectaStain; Vector Laboratories). For

coronal brain slices, brains were fixed with 4% paraformaldehyde and sectioned at 100 μm using a Leica VS1200 vibratome (Leica, Wetzlar, Germany). Slices were then washed and covered with VectaStain containing DAPI (Vector Laboratories). Images were acquired using a BZ9000 inverted fluorescent microscope (Keyence, Osaka, Japan) and digitally processed with the Keyence Analysis Software. Discrete tumor cells were identified on coronal slice images using the Neurolucida software (MBF Bioscience, Williston, VT).

Explant Culture of Coronal Brain Slices

Brains of tumor-implanted C57BL/6 mice were dissected manually and cut into 150-μm coronal slices using a Leica VS1200 vibratome (Leica). Explants were cultured on Millicell-CM culture plate inserts (Millipore) in six-well glass-bottom plates. Slices were maintained in the NSC culture medium (NSM) described previously, at 37°C in 5% CO_2/95% humidified air. Serial images were acquired every 15 minutes with a fluorescence microscope (TE2000-E; Nikon, Tokyo, Japan) and processed with MetaMorph imaging software (Universal Imaging Corp, Downingtown, PA).

Magnetic Resonance Imaging

The magnetic resonance (MR) images were acquired on a 1.5-T MR unit (MRmini SA; DS Pharma Biomedical, Osaka, Japan). T1-weighted imaging was performed using the following parameters (repetition time/echo time = 500/9 milliseconds, field of view = 20 mm, matrix = 128 × 128, slice thickness = 2 mm). Mice were anesthetized with pentobarbital and injected subcutaneously with 0.5 mM/kg Magnevist (Bayer Pharmaceuticals, Leverkusen, Germany).

Statistical Analysis

Survival analysis was performed using JMP9 (SAS Institute, Cary, NC).

Results

Genetically Modified Adult Neural Stem/Progenitor Cells Form Highly Aggressive, Malignant Brain Tumors in Immunocompetent Mice

To establish BTICs, we used two oncogenic events commonly observed in glioblastoma: deletion of the *INK4/ARF* locus and aberrant Ras activation. Alterations in the *INK4/ARF* locus can be found in approximately 50% of glioblastomas and contribute to tumorigenesis through the inactivation of the tumor suppressor gene [9,10]. Aberrant Ras activation, although seldom because of oncogenic mutations, contributes to malignant gliomas by deregulation of the RTK/Ras pathway [11,12], which is observed in more than 80% of glioblastomas [9]. A combination of *Ink4a/Arf* deletion and K-Ras overexpression in neonatal NSCs/NPCs was reported to form high-grade malignant brain tumors in mice [13], as did infection of neonatal *Ink4a/Arf* null mice with RCAS-KRas [14].

To avoid the context of developmental plasticity and signaling, we established our model using NSC/NPCs from adult *Ink4a/Arf* null mice. The NSC/NPCs were genetically modified by retroviral transduction with the constitutively active H-Ras^{V12}. Infected cells (Ras-NSCs) were GFP-, nestin-, and CD44-positive (Figure 1, *A* and *B*) and formed neurospheres from single cells (Figure 1*C*). They exhibited cellular and nuclear heterotypia (Figure 1*D*) and were able to differentiate into astrocytes, neurons, and oligodendrocytes after culture in growth factor–free, serum-supplemented medium (Figure 1*E*). Furthermore, Ras-NSCs also maintained the migratory capability of NSCs, as shown by their response to several known chemoattractants (Figure W1*A*).

Together, these results indicate that the NSC/NPCs retain their stem-like characteristics, including sphere-forming activity and trilineage differentiation ability, even after oncogenic induction.

To confirm whether Ras-NSCs can act as BTICs, we implanted 10^5 cells into the forebrain of immunocompetent mice, before their complete *in vitro* transformation. In contrast to NSC/NPCs transduced with only GFP, which did not form tumors (Figure 1*H* and Figure W1*B*), Ras-NSCs formed highly aggressive, hemorrhagic brain tumors (Figure 1, *F* and *G*) with a penetrance rate of 100% and a median survival of 4 weeks (Figure 1*H*). This result suggests that *in vivo* modulation of the Ras-NSCs further enhanced their malignant potential. As further support for this assumption, GFP-positive cells isolated from primary tumors (tumorspheres) were also serially transplantable and formed highly invasive and lethal tumors (Figure 1, *I* and *J*). Importantly, as few as 100 cells could form secondary tumors, suggesting a very high tumor-initiating ability.

Chronological Analysis of Tumor Progression Reveals an Early Onset of Tumor Cell Migration

Primary tumors closely resembled the pathologic and immunophenotypical features of human grade 4 glioma, such as hemorrhage and necrosis (Figure 2*A*), pronounced cell proliferation (Figure 2*B*), and the expression of primitive marker nestin (Figure 2*C*) and of CD44 (Figure 2*D*), reported positive in the mesenchymal subtype of glioblastoma [9]. Tumors also exhibited high cellular heterotypia (Figure 2, *E* and *F*), giant cells (Figure 2*G*), pseudopallisading (Figure 2*H*), and marked infiltration of the surrounding brain (Figure 2*I*).

To identify the onset of the main histopathologic features during tumor formation, 15 mice were implanted with Ras-NSCs and then killed and analyzed at 1-week intervals ($n = 3 \times 5$ weeks). During the first week, GFP-positive cells were clearly identifiable along the injection trajectory (Figure 3*A*). There was no mass formation or obvious hemorrhage; however, some single cells had started to migrate along fiber tracts, either laterally along the external capsule (Figure 3*B*) or medially toward the corpus callosum (Figure 3*C*), reaching as far as 400 μm into the normal brain (Figure W1*C*). During the second week, there was still no mass formation (Figure 3*D*). Most of the blood vessels close to the injection tract showed prominent encapsulation (Figure 3, *D* and *E*). This perivascular cuffing consisted of very few tumor cells, as confirmed by GFP staining (Figure 3*F*), and was mostly an accumulation of host cells, including macrophages and microglia (Figures 3*G* and W1*D*). Blood vessel encasement by reactive cells continued into the third week (Figure 3, *H* and *I*). Giant cells also appeared at this stage, with overall cellular heterotypia markedly increased (Figure 3*J*). Mass formation became obvious after 4 weeks, with tumors growing rapidly, including hemorrhage and necrosis (Figure 1*F* and Figure 2*A*), and quickly becoming lethal (Figure 1*H*).

Ras-NSCs Exhibit Multiple Invasion Patterns

As the invasion of tumor cells into the normal brain seemed to be the first notable event of tumor formation, we further investigated the onset and patterns of migration. Tumor cells spread mainly along blood vessels, fiber tracts, or into the subarachnoid space. Dissemination along blood vessels started during the first week after implantation, with tumor cells first eliciting host response, but then completely encasing the blood vessels during the mass growth stage (Figures 4*A* and

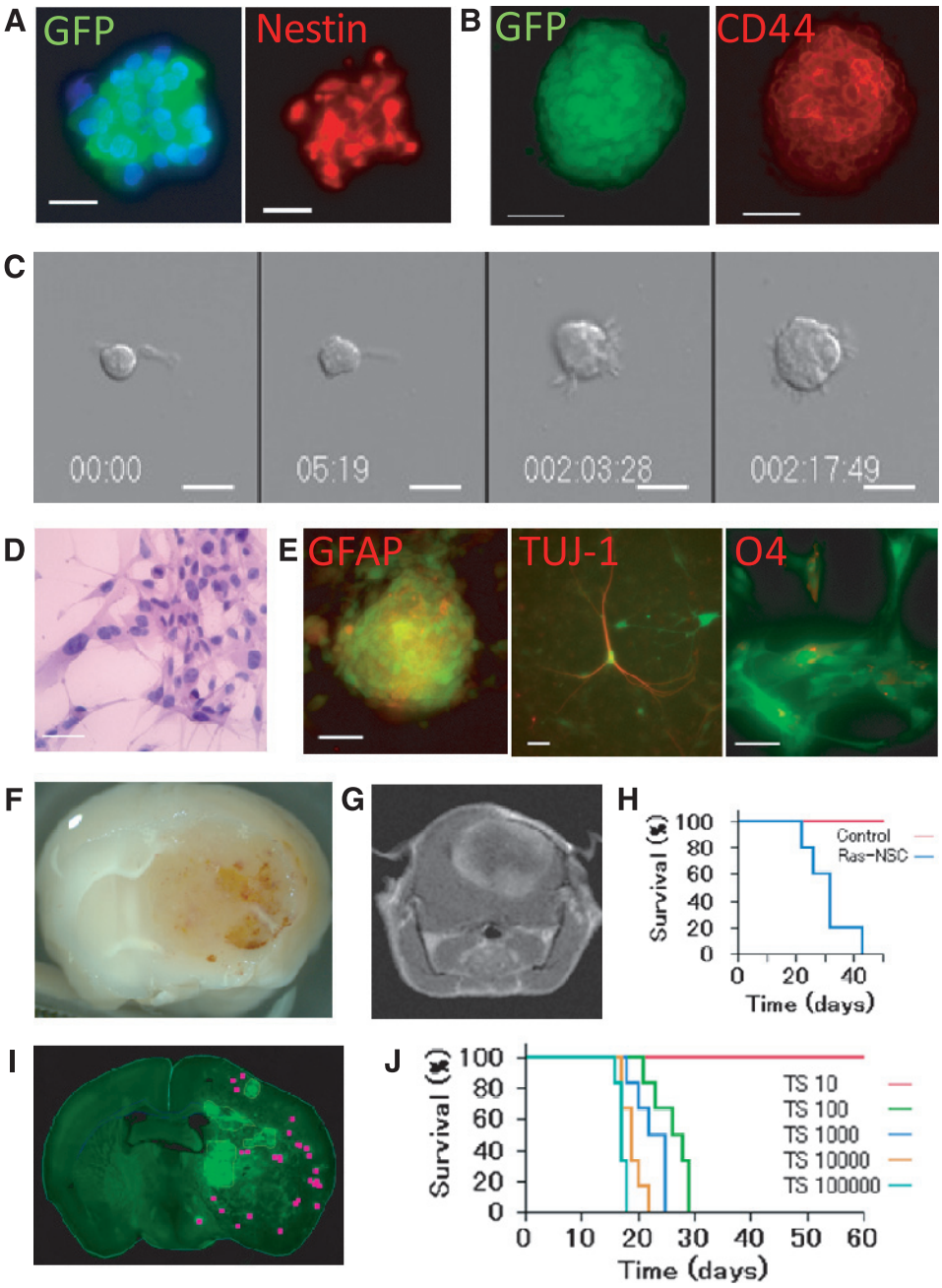

Figure 1. RAS-NSC spheres express GFP (green) and nestin (red) (A) and GFP (green) and CD44 (red) (B). Blue indicates nuclear counterstain DAPI. (C) Sequential pictures of a single Ras-NSC cell giving rise to a sphere in a soft-agar sphere formation assay. Time denotes days:hours:minutes. (D) Ras-NSCs have different sizes and morphologies. HE indicates hematoxylin-eosin staining. (E) Ras-NSCs cultured in serum-supplemented medium become positive for GFAP, Tuj-1, and O4. (F) Ras-NSCs form hemorrhagic tumors on orthotopic implantation. Mouse brain, 28 days after implantation, macroscopic coronal view at the bregma level. (G) Tumors show ring enhancement on a gadolinium-enhanced MR image. Coronal view, Gd T1-weighted image. (H) All Ras-NSC–injected mice (blue) developed brain tumors and died within 50 days after implantation. Mice injected with NSCs transduced with GFP only (control, red) did not form any tumors. Kaplan-Meier survival analysis, $n = 5$. (I) GFP-positive cells isolated from primary tumors (tumorspheres, TS) form highly invasive secondary tumors. Discrete single tumor cells or small groups of cells are marked with pink. (J) Only 100 tumor cells are required to form secondary tumors. Kaplan-Meier survival analysis of mice injected with 10^5, 10^4, 10^3, 10^2, and 10 tumor cells, $n = 6$ for each group. Scale bars, 20 μm (C); 50 μm (A, B, D, E).

W1*E*). Migration along fiber tracts was noticed as early as 2 days after implantation, showing not only single-cell movement but also an invasion pattern suggestive of collective cell migration [15] (Figure 4*B*). A third pattern consisted of tumor cells reaching the subarachnoid space and spreading over the brain surface (Figure 4*C*).

Solitary Ras-NSCs Invade Normal Parenchyma in Live Brain Slices

To confirm the migration of solitary cells during the early days after implantation, a new series of Ras-NSC–injected mice were killed every 2 days during the first week, brains were extracted,

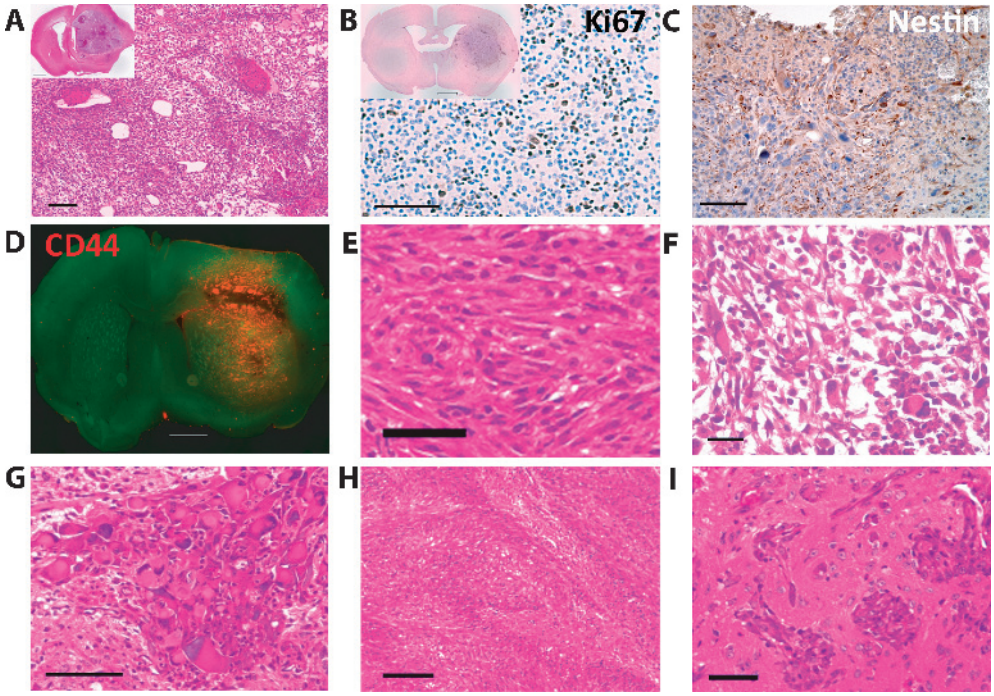

Figure 2. Histopathologic analysis of primary tumors. (A) Hemorrhage and necrosis (HE staining). Insert, whole-mount view. (B) Tumors exhibit a high proliferation index (Ki67 staining). Insert, whole-mount view. (C) Tumors are nestin- and (D) CD44-positive. Shown also are spindle-shaped (E), alveolar-like (F), and giant (G) cells. (H) Pseudopallisading. (I) Blood vessel encasement by tumor cells in the normal brain parenchyma close to the tumor border. Scale bars, 20 μm (F); 50 μm (E, I); 100 μm (A, B, C, G, H); and 1000 μm (D).

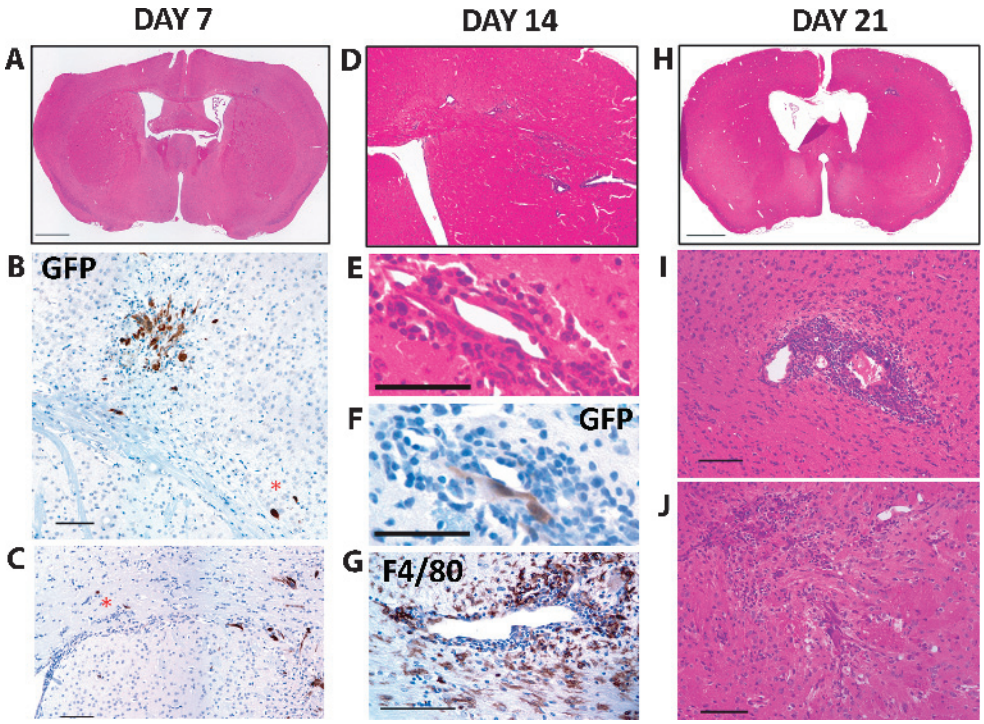

Figure 3. Chronological analysis of tumor progression. (A) Small groups of tumor cells along the injection tract, whole mount slice (HE staining), at day 7 after implantation. (B, C) GFP-positive cells, marked with an asterisk, can be observed along fiber tracts, away from the injection route. (D, E) Fourteen days after implantation, blood vessels around the injection route are encased by cells. A serial slice shows that only a few cells are GFP-positive (F), whereas many are microglia (G) (F4/80 staining). (H, I) At day 21, blood vessel encasement is still prominent. (J) Atypic cells appear around this time. Scale bars, 50 μm (E, F, G); 100 μm (B, C, I, J); and 1000 μm (A, H).

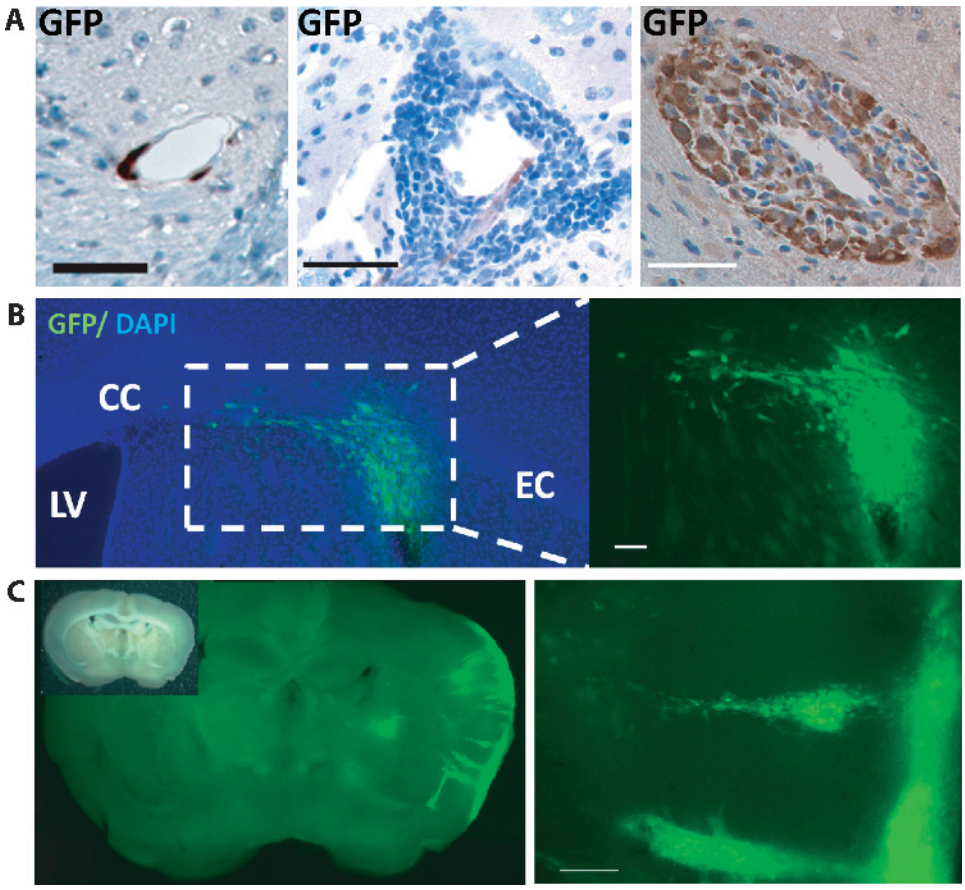

Figure 4. Invasion patterns of Ras-NSCs. (A) Left panel: A few GFP-positive tumor cells are found next to a blood vessel in the brain of a mouse killed 7 days after implantation. Middle panel: A few tumor cells and a group of host-derived cells surround a blood vessel at day 14. Right panel: A blood vessel in normal brain is surrounded by tumor cells at day 28. Scale bars, 50 μm. (B) GFP-positive tumor cells migrate along fiber tracts toward the midline. Coronal brain slice, day 2 after implantation, nuclei counterstained with DAPI. CC indicates corpus callosum; EC, external capsule; LV, lateral ventricle. Scale bar, 100 μm. (C) GFP-positive tumor cells have reached the subarachnoid space. Coronal brain slice, day 18 after implantation. Scale bar, 200 μm.

and coronal slices were cultured under video observation. Time-lapse monitoring confirmed single-cell migration at this very early stage after implantation. In contrast to NSCs without Ras activation, which did not spread from the injection site (Video W3), Ras-NSCs were highly motile as solitary infiltrative cells, exhibited repeated extension and retraction of leading processes, and sometimes reversed direction (Figure 5 and Video W1). Furthermore, once one leading cell migrated along a specific route without turning around, several cells followed it, establishing an infiltration path (Figure 6 and Video W2). The infiltrative ability of Ras-NSCs was maintained even during the later stages of tumor formation, with single cells still migrating into the normal brain in addition to the expansion of the tumor border (Video W4).

Discussion

We have established a syngeneic mouse model of a highly invasive, hypervascular, serially transplantable glioblastoma-like tumor.

One of the key features of this model is a cellular and histologic heterogeneity highly resembling that of human glioblastoma. Glioblastoma heterogeneity has traditionally been attributed to a gradual accumulation of diverse genetic events [16,17]. Recently, the existence of glioma stem cells [18], which can give rise to different types of daughter cells, has been proposed as another cause of cellular diversity [19,20].

Our model uses two genetic switches: Ras overexpression and *Ink4a/Arf* deletion. However, implantation of the NSC/NPC population before complete *in vitro* transformation is intended to allow further genetic and/or epigenetic events to occur *in vivo*, a process that is thought to occur during spontaneous gliomagenesis in human patients. Despite being genetically modified, these cells retain some of the properties of normal NSC/NPCs as shown by their ability to differentiate *in vitro* despite Ras overexpression. Retaining normal stem cell features also provides Ras-NSCs with inherent motility and susceptibility to chemical cues from the environment [21–23]. Furthermore, NSCs' characteristics might enhance tumorigenic ability and probably also contribute, as intended, to the cellular heterogeneity. The use of adult NSC/NPC as initial cells complements similar models that rely on neonatal NSC/NPCs [13], ES cells [24], or model the progression of low grade astrocytoma to secondary glioblastoma [12]. In the future, it will be interesting to isolate different types of cells, such as giant cells, from live tumor-bearing brain slices and to analyze their genetic signature, differentiation status, and clonal tumorigenic potential.

Another merit of our model is its predictable and reproducible growth pattern. After orthotopic implantation, genetically modified adult NSC/NPCs stably form short-latency tumors. *In vivo* growth characteristics showed remarkable consistency and allowed detailed histopathologic analysis from the early stages of tumor development and throughout the course of the disease.

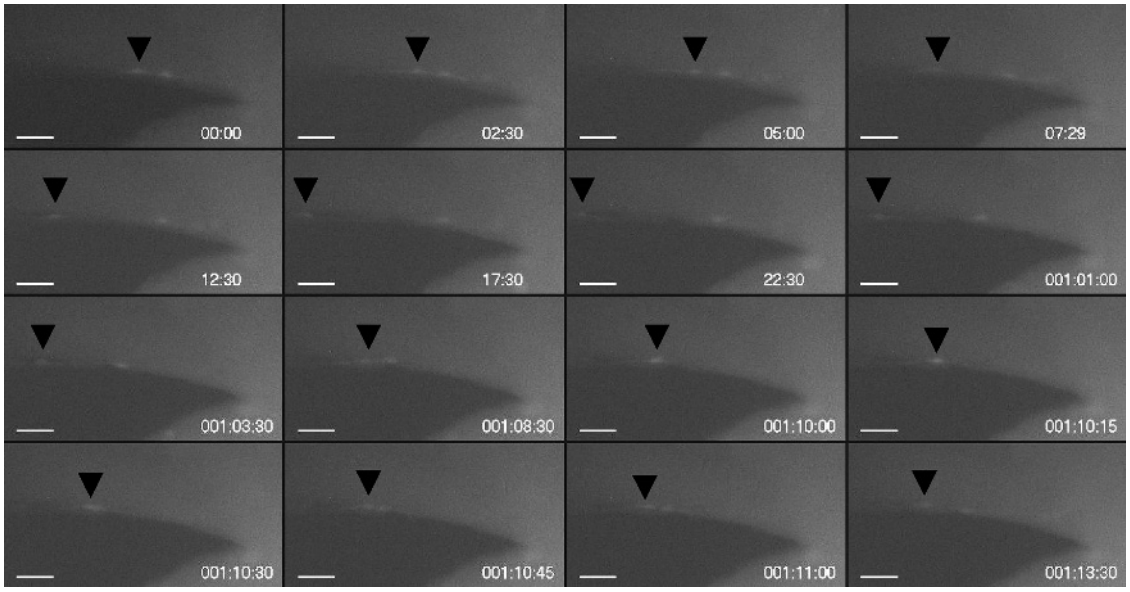

Figure 5. Tumor cells moving along the wall of the lateral ventricle. Sequential pictures of GFP-positive tumor cells moving within a brain slice in culture. Arrowhead indicates cell changing direction. Time denotes days:hours:minutes. Scale bar, 30 μm.

The key finding of our analysis was that Ras-NSCs migrated along fiber tracts, blood vessels, and into the subarachnoid space and that migration along fiber tracts and blood vessels began long before tumor mass formation. The three main dissemination routes observed in our study are consistent with classic reports based on postmortem analysis of human gliomas [25,26], validating this model as a tool for invasion analysis. Onset of migration has usually been linked to the lack of oxygen and nutrients that is inherent to tumor growth. Our results show that neoplastic cells are able to initiate invasion even in the absence of such environmental pressure. Movement along fiber tracts might be the result of an affinity for stiff structures, as has been shown for breast tumor cells [27]. It might also reflect a pattern of collective cell migration, with paths of least mechanical resistance created by individual "leader" cells, as seen with invasive cancer cells such as fibrosarcoma [28].

Intraparenchymal movement of the tumor cells might also be the result of chemoattractant cues from the SVZ stem cell niche or the environment. Indeed, our Ras-NSCs responded to addition of EGF in chemotaxis assays; however, their poor response to several other

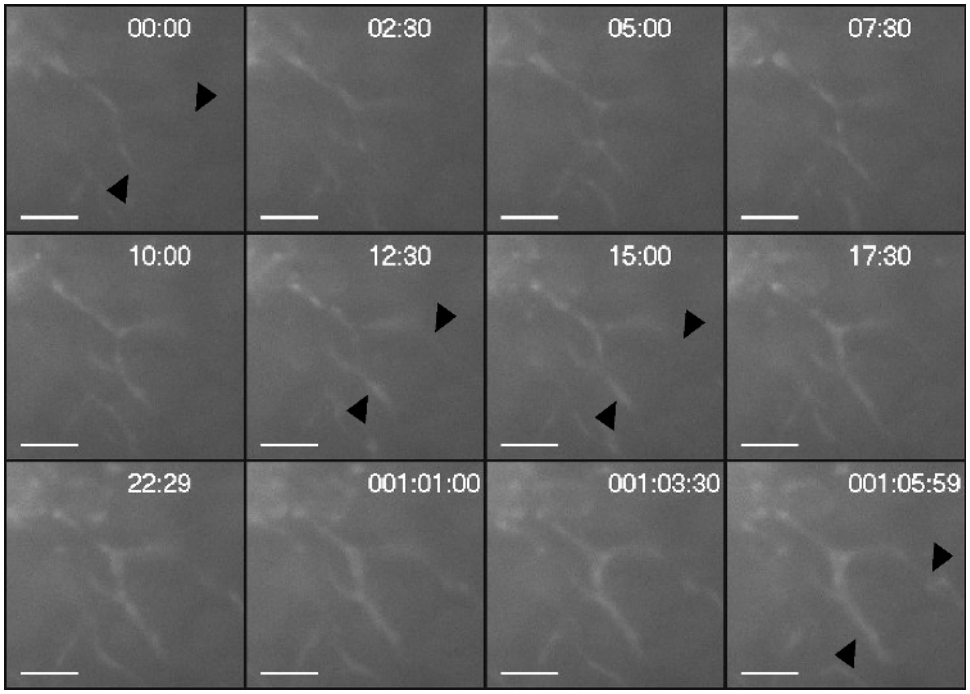

Figure 6. Tumor cells form infiltration paths in the normal brain parenchyma. Sequential pictures of GFP-positive tumor cells moving within a brain slice in culture. Arrowheads indicates gradual formation of infiltration paths. Time denotes days:hours:minutes. Scale bar, 30 μm.

known chemoattractants suggests that *in vivo* invasion may be regulated by a yet unknown factor, might depend on the brain matrix for modulation, or might require a combination of chemokines.

Affinity for blood vessels seems to be independent of oxygen gradients because cultured brain slices do not have blood circulation but could be caused by endothelium-secreted factors or cues from perivascular niches. Interestingly, injection of rat cells into neonatal rat brains has also been reported to result in prompt initiation of invasion; however, the immortalized glioma cells migrated exclusively along blood vessels [29].

Performing the analysis with primary cells in a syngeneic model has allowed us to explore intraparenchymal infiltration, which has not been well studied in live systems. Video monitoring of GFP-expressing cells in brain slices confirmed that solitary Ras-NSCs started migrating within days of implantation. The first cells to leave the injection site exhibited relatively random dynamics, stopping, and turning, as if responding to environmental cues. However, once these leading cells chose a route, they established a path for other cells. Although it is still unclear whether these early migrating cells are able to survive and proliferate at the distant sites they reach, the paths that they create may serve as dissemination routes during later stages or as recurrence sites during treatment. Isolating such "leader" cells from brain slices and identifying their characteristic markers, as well as the molecular base of their path-forming capability will likely advance not only prognostic determination but also treatment strategies.

Current anti-invasion therapies for malignant gliomas include targeting the tumor cell–matrix interaction, such as the use of integrin antagonists and MMP inhibitors, have shown promise *in vitro*, and some are now in clinical trials [30]. However, intrinsic characteristics of glioma cells must also be considered. Although all malignant glioma cells are believed to have an infiltrative ability, a transient or permanent mesenchymal phenotype or the presence of such a subgroup in a tumor has been reported to result in increased invasiveness. Targeting this phenotype or preventing new cells from acquiring it through the use of inhibitors of the epithelial-mesenchymal transition could be another therapeutic strategy, which we also plan to test in our model. Taken together, our results highlight a pronounced intravascular, intraparenchymal, and subpial tumor cell migration preceding mass formation in the adult brain, suggesting the need for early and sustained anti-invasion therapy.

Acknowledgments

The authors thank Y. Matsuzaki and S. Suzuki (Keio University) for flow cytometry cell sorting, I. Ishimatsu for preparing pathology samples, and K. Arai for secretarial assistance.

References

[1] Holland EC (2001). Gliomagenesis: genetic alterations and mouse models. *Nat Rev Genet* **2**, 120–129.

[2] Kamnasaran D (2009). Stem cells and models of astrocytomas. *Clin Invest Med* **32**, E166–E179.

[3] de Vries NA, Beijnen JH, and van Tellingen O (2009). High-grade glioma mouse models and their applicability for preclinical testing. *Cancer Treat Rev* **35**, 714–723.

[4] Bao S, Wu Q, McLendon RE, Hao Y, Shi Q, Hjelmeland AB, Dewhirst MW, Bigner DD, and Rich JN (2006). Glioma stem cells promote radioresistance by preferential activation of the DNA damage response. *Nature* **444**, 756–760.

[5] Holland EC, Celestino J, Dai C, Schaefer L, Sawaya RE, and Fuller GN (2000). Combined activation of Ras and Akt in neural progenitors induces glioblastoma formation in mice. *Nat Genet* **25**, 55–57.

[6] Llaguno S, Chen J, Kwon CH, Jackson EL, Li Y, Burns DK, Alvarez-Buylla A, and Parada LF (2009). Malignant astrocytomas originate from neural stem/progenitor cells in a somatic tumor suppressor mouse model. *Cancer Cell* **15**, 45–56.

[7] Maeda T, Hobbs RM, Merghoub T, Guernah I, Zelent A, Cordon-Cardo C, Teruya-Feldstein J, and Pandolfi PP (2005). Role of the proto-oncogene *Pokemon* in cellular transformation and ARF repression. *Nature* **433**, 278–285.

[8] Morita S, Kojima T, and Kitamura T (2000). Plat-E: an efficient and stable system for transient packaging of retroviruses. *Gene Ther* **7**, 1063–1066.

[9] Cancer Genome Atlas Research Network (2008). Comprehensive genomic characterization defines human glioblastoma genes and core pathways. *Nature* **455**, 1061–1068.

[10] Schmidt EE, Ichimura K, Reifenberger G, and Collins VP (1994). CDKN2 (p16/MTS1) gene deletion or CDK4 amplification occurs in the majority of glioblastomas. *Cancer Res* **54**, 6321–6324.

[11] Guha A, Feldkamp MM, Lau N, Boss G, and Pawson A (1997). Proliferation of human malignant astrocytomas is dependent on Ras activation. *Oncogene* **15**, 2755–2765.

[12] Shannon P, Sabha N, Lau N, Kamnasaran D, Gutmann DH, and Guha A (2005). Pathological and molecular progression of astrocytomas in a GFAP:12 V-Ha-Ras mouse astrocytoma model. *Am J Pathol* **167**, 859–867.

[13] Tamase A, Muraguchi T, Naka K, Tanaka S, Kinoshita M, Hoshii T, Ohmura M, Shugo H, Ooshio T, Nakada M, et al. (2009). Identification of tumor-initiating cells in a highly aggressive brain tumor using promoter activity of nucleostemin. *Proc Natl Acad Sci USA* **106**, 17163–17168.

[14] Uhrbom L, Dai C, Celestino JC, Rosenblum MK, Fuller GN, and Holland EC (2002). Ink4a-Arf loss cooperates with KRas activation in astrocytes and neural progenitors to generate glioblastomas of various morphologies depending on activated Akt. *Cancer Res* **62**, 5551–5558.

[15] Friedl P and Gilmour D (2009). Collective cell migration in morphogenesis, regeneration and cancer. *Nat Rev Mol Cell Biol* **10**, 445–457.

[16] Biernat W, Tohma Y, Yonekawa Y, Kleihues P, and Ohgaki H (1997). Alterations of cell cycle regulatory genes in primary (*de novo*) and secondary glioblastomas. *Acta Neuropathol* **94**, 303–309.

[17] Bredel M, Scholtens DM, Harsh GR, Bredel C, Chandler JP, Renfrow JJ, Yadav AK, Vogel H, Scheck AC, Tibshirani R, et al. (2009). A network model of a cooperative genetic landscape in brain tumors. *JAMA* **302**, 261–275.

[18] Singh SK, Clarke ID, Terasaki M, Bonn VE, Hawkins C, Squire J, and Dirks PB (2003). Identification of a cancer stem cell in human brain tumors. *Cancer Res* **63**, 5821–5828.

[19] Huse JT and Holland EC (2010). Targeting brain cancer: advances in the molecular pathology of malignant glioma and medulloblastoma. *Nat Rev Cancer* **10**, 319–331.

[20] Reya T, Morrison SJ, Clarke MF, and Weissman IL (2001). Stem cells, cancer, and cancer stem cells. *Nature* **414**, 105–111.

[21] Cayre M, Canoll P, and Goldman JE (2009). Cell migration in the normal and pathological postnatal mammalian brain. *Prog Neurobiol* **88**, 41–63.

[22] Aboody KS, Brown A, Rainov NG, Bower KA, Liu S, Yang W, Small JE, Herrlinger U, Ourednik V, Black PM, et al. (2000). Neural stem cells display extensive tropism for pathology in adult brain: evidence from intracranial gliomas. *Proc Natl Acad Sci USA* **97**, 12846–12851.

[23] Ehtesham M, Yuan X, Kabos P, Chung NH, Liu G, Akasaki Y, Black KL, and Yu JS (2004). Glioma tropic neural stem cells consist of astrocytic precursors and their migratory capacity is mediated by CXCR4. *Neoplasia* **6**, 287–293.

[24] Ding H, Roncari L, Shannon P, Wu X, Lau N, Karaskova J, Gutmann DH, Squire JA, Nagy A, and Guha A (2001). Astrocyte-specific expression of activated p21-*ras* results in malignant astrocytoma formation in a transgenic mouse model of human gliomas. *Cancer Res* **61**, 3826–3836.

[25] Matsukado Y, Maccarty CS, and Kernohan JW (1961). The growth of glioblastoma multiforme (astrocytomas, grades 3 and 4) in neurosurgical practice. *J Neurosurg* **18**, 636–644.

[26] Arita N, Taneda M, and Hayakawa T (1994). Leptomeningeal dissemination of malignant gliomas. Incidence, diagnosis and outcome. *Acta Neurochir (Wien)* **126**, 84–92.

[27] Levental KR, Yu H, Kass L, Lakins JN, Egeblad M, Erler JT, Fong SF, Csiszar K, Giaccia A, Weninger W, et al. (2009). Matrix crosslinking forces tumor progression by enhancing integrin signaling. *Cell* **139**, 891–906.

[28] Friedl P and Wolf K (2008). Tube travel: the role of proteases in individual and collective cancer cell invasion. *Cancer Res* **68**, 7247–7249.

[29] Farin A, Suzuki SO, Weiker M, Goldman JE, Bruce JN, and Canoll P (2006). Transplanted glioma cells migrate and proliferate on host brain vasculature: a dynamic analysis. *Glia* **53**, 799–808.

[30] Reardon DA, Fink KL, Mikkelsen T, Cloughesy TF, O'Neill A, Plotkin S, Glantz M, Ravin P, Raizer JJ, Rich KM, et al. (2008). Randomized phase II study of cilengitide, an integrin-targeting arginine-glycine–aspartic acid peptide, in recurrent glioblastoma multiforme. *J Clin Oncol* **26**, 5610–5617.

Supplemental Information

Methods

In vitro *migration assay*. Random cell migration in response to several chemoattractants was quantified using the agarose drop assay [1]. Neural stem cells transduced with GFP only or Ras-NSCs were suspended in DMEM/F12 containing B27 supplemented with 0.3% low-melting point agarose (Sigma) at a density of 10^7 cells/ml. Drops of 1.5 μl of this suspension were placed at the center of poly-L-lysine–coated glass-bottom 24-well plates and then maintained at 4°C for 15 minutes until the agarose hardened. Drops were then covered with either DMEM/F12 containing B27 alone (control), or supplemented with the following factors: EGF, FGF, PDGFB, VEGF, CXCL12, IGF-1 at 50 ng/ml, 20 ng/ml IL-6, NSM and 10% fetal calf serum, each added to two wells. Time-lapse recording of the cells migrating out of the agarose drop was performed for 46 hours with a fluorescence microscope (TE2000-E; Nikon). Experiments were performed in duplicate and migration was quantified using the MetaMorph software, by measuring the migrated distance of 15 leading cells from at least three independent wells. Data were analyzed for statistical significance by the Wilcoxon signed-rank test, and $P < .01$ was considered statistically significant.

Quantification of pathology samples. For the chronological weeks 1 to 4 analysis, at least two paraffin slices from at least two different mice were used for quantification for each time point. For quantification of invasion, the distance between the tumor margin (or margin of the biggest group of tumor cells for early stage) and five invasive tumor cells/sample was measured from GFP-stained paraffin slices. For microglia accumulation, the percentage of the F4/80–positive area in the injected hemisphere was calculated. Tumor cells associated with blood vessels within the normal brain were counted from GFP-stained slices. All measurements were performed with the Keyence analysis software. Results were expressed as mean ± SEM.

Reference

[1] Varani J, Orr W, and Ward PA (1978). A comparison of the migration patterns of normal and malignant cells in two assay systems. *Am J Pathol* **90**, 159–172.

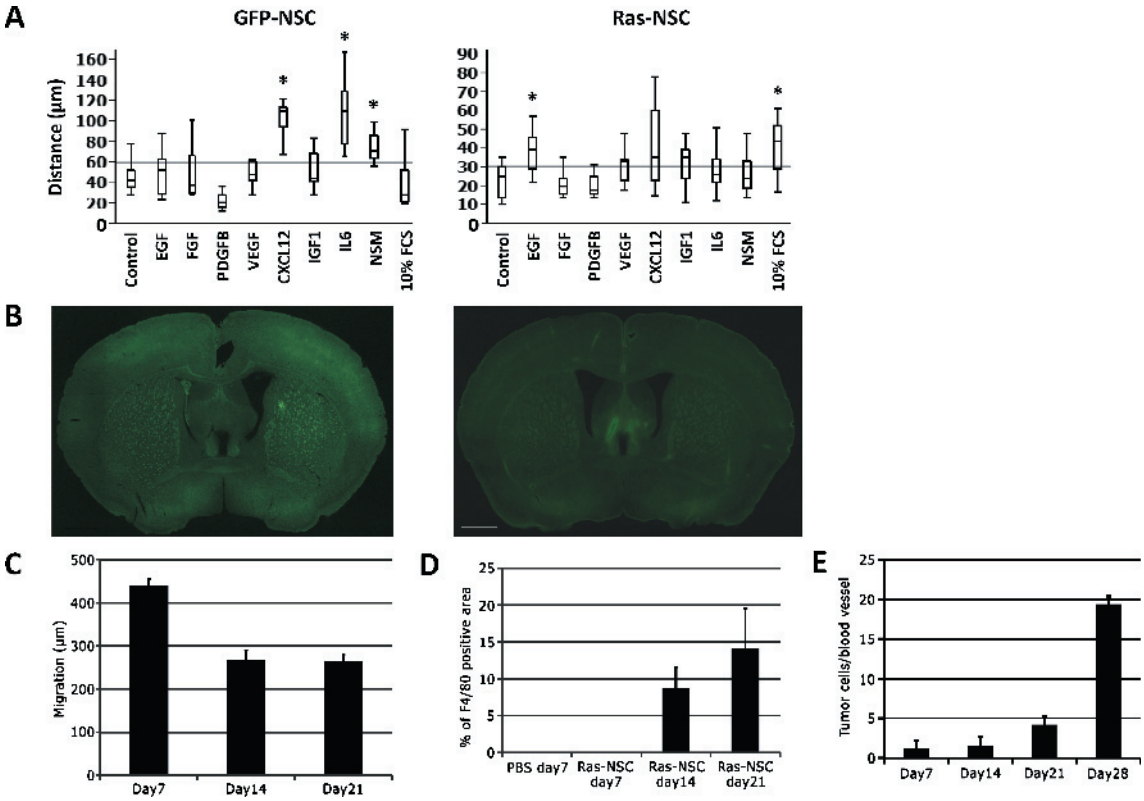

Figure W1. (A) In the *in vitro* migration assay, NSCs transduced with GFP only respond to CXCL12, IL-6, and NSM, whereas Ras-NSCs are attracted by EGF and serum. CXCL12 indicates chemokine (C-X-C motif) ligand 12; EGF, epidermal growth factor; FGF, basic fibroblast growth factor; IGF-1, insulin-like growth factor 1; IL-6, interleukin 6; PDGFB, platelet-derived growth factor β; VEGF, vascular endothelial growth factor. *$P < .01$ compared with control group. (B) NSCs transduced with GFP only do not form tumors when implanted into syngeneic mice. Left panel: Brain slice showing few residual cells at the injection site 11 days after implantation of 10^5 cells. Right panel: At day 14 after implantation, no residual cells can be identified. (C) Chronological quantification of solitary tumor cells infiltration into the normal brain. Invasion of Ras-NSCs is prominent from the first week after implantation. (D) Starting the second week after implantation, F4/80–positive microglia start to accumulate around the injection site. There is no obvious microglia accumulation after injection of phosphate-buffered saline only. (E) GFP-positive tumor cells associated with blood vessels drastically increase in number during the final stage of tumor formation.

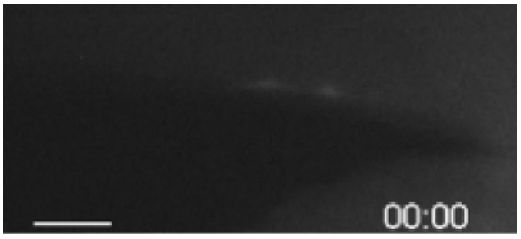

Video W1. GFP-positive tumor cells moving along the wall of the lateral ventricle within a brain slice in culture. Time denotes days: hours:minutes. Scale bar, 30 μm. All files are in AVI format. It is preferable to use QuickTime for replaying all movies.

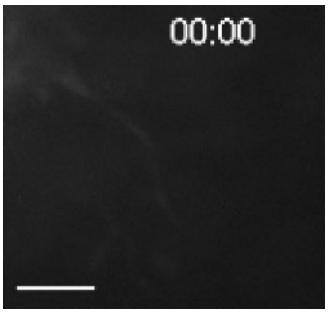

Video W2. GFP-positive tumor cells form infiltration paths in the normal parenchyma of a brain slice in culture. Time denotes days: hours:minutes. Scale bar, 30 μm.

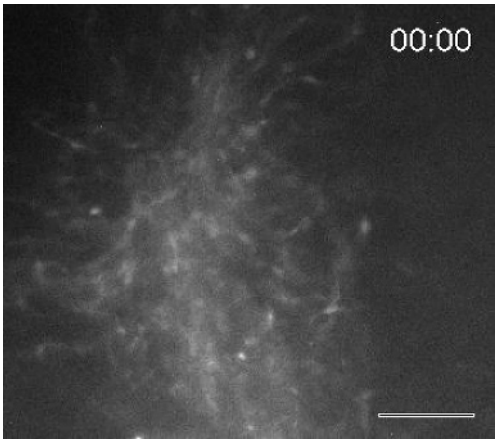

Video W3. GFP-positive NSCs move within the group of cells at the injection site but do not infiltrate into the normal brain. Time denotes days:hours:minutes. Scale bar, 50 μm.

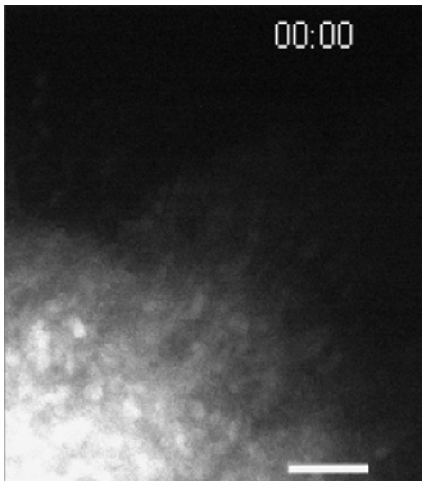

Video W4. At the stage when a tumor mass has been formed, tumor both expands and infiltrates the surrounding brain. Time denotes days:hours:minutes. Scale bar, 100 μm.